ELSEVIER

Journal of Nuclear Materials 266–269 (1999) 691–696

journal of nuclear materials

# Simulation of transient wall pumping, fuelling effects and density control in tokamaks

M. Sugihara [a,*], G. Federici [a], C. Grisolia [b], P. Ghendrih [b], J.T. Hogan [c], G. Janeschitz [a], G. Pacher [d], D.E. Post [a]

[a] *c/o MPI fur Plasmaphysik, ITER JWS Garching Co-center, Boltzmannstraße 2, 85748 Garching, Germany*
[b] *Association EURATOM-CEA sur la fusion, C.E. Cadarache, France*
[c] *Oak Ridge National Laboratory, Oak Ridge, TN 37830, USA*
[d] *Centre canadien de fusion magnétique, Varennes, Québec, Canada*

**Abstract**

A dynamical model has been developed which solves a time-dependent coupled system of equations for the (1) plasma density and (2) hydrogenic concentrations in the implantation layer of several representative plasma facing/limiting walls in tokamaks in order to examine the density behaviour during the transient phase of discharges as well as long pulse discharges, which are dominated by the wall pumping/fuelling characteristics. A 1-D plasma particle transport code including a model for the SOL and an analytical neutral transport model has been used to describe the plasma particle transport processes. The Local Mixing Model with some adaptations has been used to describe the behaviour of the hydrogenic concentrations in the walls. The new model significantly improves the simulation of a Tore Supra experiment with a transition from limiting the plasma on the outer limiter to limiting the plasma on the inner wall compared our previous, more simple model. Long pulse discharges in Tore Supra are examined by the more simplified model to identify the dominant mechanisms for the constant particle absorption mechanisms. 

*Keywords:* Hydrogen retention; ITER; Particle control; Particle transport; Tore Supra; Wall absorption; Wall fuelling; Wall pumping

## 1. Introduction

The material surfaces of the components surrounding the core and the divertor plasmas in tokamaks play an important role in controlling the plasma density and determining the external fuelling and pumping requirements during the various transient phases of a discharge. Pumping and fuelling effects of the walls will also affect the overall DT fuel cycle and the particle balance of next step DT fuelled tokamaks such as ITER. Although details of these processes are very complicated, it is necessary to estimate the global characteristics of the process for a wide range of operation scenarios in ITER. A simplified modelling approach to analyse the retention of hydrogenic species, the associated density behaviour and its dependence on various operational parameters are needed and must be validated against the existing tokamak experiments.

For this purpose, a dynamical model has been developed, which solves a time-dependent coupled system of equations for (1) plasma density and (2) hydrogenic concentrations in the implantation layer of the representative walls. A 0-D plasma model coupled with a simple saturation model for graphite wall has been previously developed to examine the wall absorbing characteristics and the associated global plasma density behaviour with simplified assumptions on the particle flux onto the wall [1]. Although the global feature of the time behaviour of plasma density in Tore Supra transition experiments from outer limiter to inner wall was

* Corresponding author. Tel.: +49 89 3299 4120; fax: +49 89 3299 4110; e-mail: sugiham@sat.ipp-garching.mpg.de

0022-3115/99/$ – see front matter 
PII: S0022-3115(98)00677-1

reproduced reasonably well by this model, some adjustment of particle confinement time (or particle flux to each wall) during the discharge phases were necessary. In addition, somewhat arbitrary assumptions on the interacting volume with the particles were used, since the correct estimation of the penetration depth of the implanted particles needs detailed calculations on neutrals and plasma temperatures.

In order to improve the model further, we have developed a 1-D plasma particle transport model coupled with the wall model based on the Local Mixing Model [2] for graphite wall. Together with this model extension, we will use the various results of the experimental and numerical analyses on this experiment performed so far [3–5] to supplement the still uncertain information, e.g., penetration depth of the implanted particles. Using the extended model and these informations, we will re-examine the Tore Supra transition experiments. Based on this re-examined result, we will also identify under what conditions the previous models can still be applicable. As an example of this applicable discharge condition, we will examine long pulse quasi-steady discharges performed in Tore Supra, where plasma conditions are almost constant, with the previous simple model.

## 2. Plasma and wall models

We describe here the plasma and wall models with emphasis on the newly extended part from the previous model [1]. In the previous model, we have employed the 0-D plasma model, in which the total particle flux $f$ is given by $N_p/\tau_p$ ($N_p$, total plasma particles; $\tau_p$, particle confinement time;) and the particle fluxes onto each walls (first wall and limiter) are partitioned from this total flux (partition fraction is taken from Refs. [6,7]). For the wall model for graphite based materials, we have employed a simplified saturation model, in which the time behaviour of the particle concentration $N_c^j$ in the $j$th wall is expressed by $dN_c^j/dt = \phi^j(1 - N_c^j/N_{max}^j)$ ($N_{max}^j$; saturation concentration in graphite $j$th wall). With this rather simplified model, it has been demonstrated that the time behaviour of plasma density in Tore Supra transition experiments from outer limiter to inner wall [3,4] was reproduced reasonably well [1]. However, some shortcomings to simulate this transition experiment by this model have also been recognised. The most difficult point was a large change of absorbing characteristics by the walls after the gas-puff termination from those of during the gas puff phase. In fact, in the experiment, walls still absorb large amounts of recycled and fuelled particles (fuelling efficiency is ≈10–20%) during the gas-puff phase, while after gas-puff termination, the decay rate of plasma density becomes fairly low. In order to reproduce this density behaviour by the previous model, $\tau_p$ had to be increased significantly (factor of five) after the gas puff termination.

It is natural to expect that this difficulty could be improved substantially by employing more realistic plasma and wall models. First of all, it seems reasonable that the particle flux be reduced much more pronouncedly than that of average density when the plasma density starts to reduce after gas-puff termination due to the rapid reduction of the scrape-off layer density (profile effect). Secondly, when the particle flux to the highly exposed wall is reduced, the particle desorption will take place, which retards the decay of plasma density somewhat. These are the motivations of the present extension of the previous models. Furthermore, various analysis results for these experiments have been accumulated, and thus we try to make the most of these results for the present model extension.

First in order to evaluate the plasma profile effect correctly, instead of a 0-D plasma model, we solve the following 1-D particle transport equation including the parallel loss term in the SOL region.

$$\frac{\partial n_p}{\partial t} = \frac{\partial}{\partial r}\left(D\frac{\partial n_p}{\partial r} - n_p v_{in}\right) + S_n(r) - \frac{n_p}{\tau_{\|}}U(a, r_w), \tag{1}$$

where $D$, $v_{in}$ and $S_n(x)$ are the diffusion coefficient, inward pinch velocity and the source term from neutral ionisation and charge exchange, respectively. $U(a, r_w)$ is unity only between $a$ and $r_w$, which is SOL region ($r_w$, radius of wall), and is zero outside of this range. $\tau_{\|}$ is the particle loss time along the open field line intersecting with the limiter, which is expressed as $\tau_{\|} = L/v_{\|}^{SOL}$ in terms of the connection length $L = \pi qR$ ($q$; safety factor, $R$; major radius) and the parallel velocity $v_{\|}^{SOL} = 0.3C_v$ ($C_v(T_s)$; sound velocity). Here we have assumed 0.3 for the coefficient, which is within the range of experimental and numerical evaluation for the flow velocity in SOL region. Since we will not solve the energy equations in this model, the ion temperature $T_s$ in the SOL region is estimated from the convective power flow to the limiter ($P_{sol} = 7.8n_sT_s^{1.5}$; $n_s$ is the density in SOL) by using the estimated power flow to the SOL region $P_{sol}$. Particle fluxes to the limiter and the first wall are given by

$$\frac{n_p(r)}{\tau_{\|}}V_{SOL}(r) \quad \text{(limiter)}, \tag{2}$$

$$D\frac{\partial n_p(r)}{\partial r}\bigg|_{r=r_w} S_{pl} \quad \text{(first wall)}, \tag{3}$$

where $V_{SOL}(r)$ and $S_{pl}$ are the volume of the SOL and the plasma surface area, respectively. The source term $S_n(r)$ is calculated using the analytical form of the neutral profile in slab geometry through ionisation and charge exchange [8]. The source profile inside and near the SOL region is sensitive to the birth place of neutrals, which eventually affects the particle flux to the limiter and the first wall significantly. Thus, the overall neutral profile is calculated by superimposing each of the profiles for the neutrals starting from each of the mesh point of the

limiter or the first wall. Spatial profile of both diffusion coefficient and inward pinch velocity are assumed to be parabolic across the plasma. If the spatial profile of $D$ and $v_{in}$ are assumed the same, it is well known that the same density profile can be produced by arbitrary combination of $D$ and $v_{in}$, so that we will assume zero inward pinch velocity for simplicity in the simulation.

For the wall model, an appropriate description of the particle desorption must be included for the improvement of the previous model. Thus, we use the model based on the local mixing model [2], which has been used to examine the PTE experiments in JET [9] and desorption/conditioning characteristics in Tore Supra [10]. The basic equations are

$$\frac{\partial C_s}{\partial t} = D_c\left(\frac{\partial^2 C_s}{\partial x^2}\right) + \phi U(0,\Delta_i)/\Delta_i - \gamma C_s^2 - \frac{\partial C_t}{\partial t}, \quad (4)$$

$$\frac{\partial C_t}{\partial t} = \frac{1}{\tau_a} C_s\left(1 - \frac{C_t}{C_{max\,0}}\right) - \frac{1}{\tau_a}\beta C_t - \sigma\phi U(0,\Delta_i)C_t, \quad (5)$$

where $C_s$ and $C_t$ are solute and trapped concentration in the wall, respectively. $D_c$, $\gamma$, $\beta$, $\sigma$ are the diffusion, volume recombination, thermal detrapping coefficients and particle-induced detrapping cross section, respectively. $\tau_a$ and $C_{max\,0}$ are the time constant for the trapping and detrapping process and the maximum trapped concentration in the wall, respectively. All of the numerical values of these constants and coefficients are taken from Refs. [5,10]. This system of Eqs. (4) and (5) is solved for several representative plasma facing and limiting walls. They are (i) general first wall, which receives the particle flux of Eq. (3), (ii) first wall near the gas puff port, (iii) limiter, which receives the particle flux of Eq. (2). In the present paper, we will somewhat simplify this model by neglecting the diffusion into bulk of the materials of Eq. (4), when the discharge time duration is $\approx$10 s, which is too short for the diffusion term to be effective. Estimation of the penetration depth $\Delta_i$ requires the incident energy of the particles by solving the plasma energy equation, which is not the case in the present paper. Thus, we will estimate $\Delta_i$ separately from the detailed Monte Carlo calculation of the charge exchange implantation source [5] for the experiments to be analysed. Furthermore, we will assume a uniform particle deposition profile inside this penetration depth as inferred in this Monte Carlo calculation.

Particle influx to each wall from the plasma are provided by Eqs. (2) and (3) by solving the plasma equation Eq. (1). Then the desorbed particle flux from the walls are evaluated by solving Eqs. (4) and (5), which, together with the gas-puffing, provide the particle source term for Eq. (1). In this way, Eqs. (1)–(5) are solved simultaneously with appropriate initial conditions for each walls.

## 3. Simulation of Tore Supra transition experiments

We apply the developed model to the Tore Supra transition experiments from the outer limiter to the inner wall [3,4] and examine how it has improved from the previous model. This experiment has been performed with CFC wall materials after long hours of wall conditioning. Plasma is initiated on the outer limiter and the density is increased by gas puff. Then, the gas puff is terminated and the plasma stayed on the outer limiter with a density decay for a few seconds. After that, the plasma is shifted to the inner wall, at which the plasma density drops quickly. These sequences of discharges are repeated 15 times with a dwell time of 600 s. Detailed Monte Carlo neutral calculations have been done by using the measured Thomson profiles for plasma density and temperature for all the shots (shot 5068–5085) of this experimental sequence [5]. Fig. 1 shows the charge exchange implantation source profile for the first (5068) and the last (5085) shot in the sequence. It is shown that, during the sequence, the penetration depth decreases, since the edge density increases and edge ion temperature decreases as the wall tends to saturate. This result provides the basis for the choice of the penetration depth $\Delta_i$ in the model. Here we select two particular shots (5070, 5080) for the simulation. From Fig. 1, we estimate $\Delta_i \approx 30$ nm for shot 5070 and $\Delta_i \approx 20$ nm for shot 5080. We use $\approx$12 m$^2$ for the total interacting area, which is estimated by the $H_\alpha/D_\alpha$ measurement in the experiment.

We examine the plasma diffusion coefficient and the inward pinch velocity by comparing the resultant density profile with the Thomson measured profile in the experiment. Fig. 2 shows the calculation result with the diffusion coefficient of

$$D(r) = 0.15(1 + (r/a^2) \quad (m^2/s) \quad (6)$$

and the zero inward velocity at $t = 3.5$ s (near gas-puff termination) for shot 5070. It is seen that the spatial profile of Eq. (6) (together with the neutral penetration

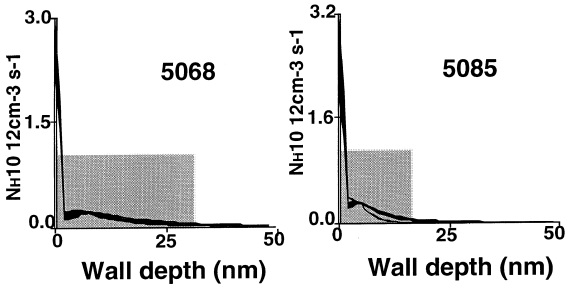


Fig. 1. Charge exchange implantation profile calculated by Monte Carlo neutral transport code using the experimentally observed Thompson profiles of density and temperature for shot 5068 (first shot of sequence) and 5085 (final shot).

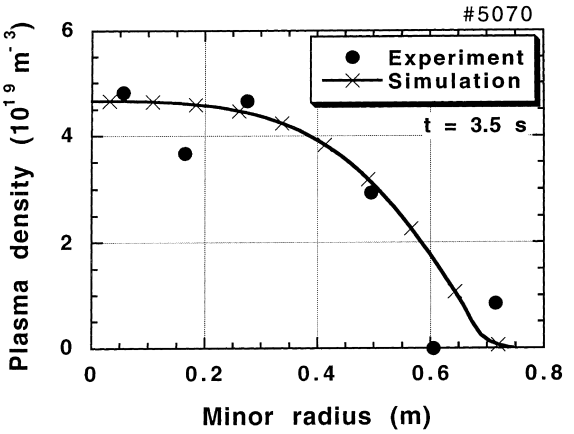


Fig. 2. Density profile by simulation (solid line with crosses) with the diffusion coefficient of Eq. (6) and zero inward pinch velocity at $t = 3.5$ s for shot 5070. Closed circles show the experimental measurement by Thomson scattering.

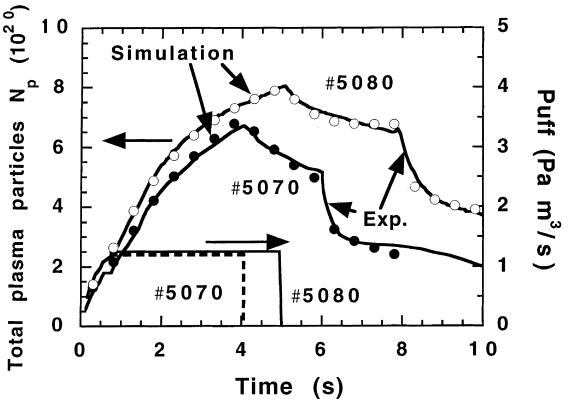


Fig. 3. Best fitted simulation results by the present extended model for shot 5070 (solid circles) and 5080 (open circles) and their experimental time behaviours (solid lines). Also shown are gas puff rate for 5070 (dotted line) and 5080 (solid line).

model) can reproduce the measured density profile reasonably well.

Initial particle concentration in each of the walls is important to reproduce the time behaviour of plasma particles, though this information is limited. Some supportive indications are available from the experimental analyses for desorption after discharge using Eqs. (4) and (5) [10]. In Ref. [10], it has been identified that the initial values for solute concentration $C_s$ are very small, and only small fraction of the particles deposited in the wall per shot is left in the wall at the end of one cycle of this sequence. Based on these informations, we set the initial values of $C_s$ arbitrarily low and $C_t \approx 0.6$ of the saturation concentration at the experimental wall temperature of 190°C and adjust these values to reproduce the experimental time behaviour of plasma density. The plasma diffusion coefficient is also adjusted to obtain the best fit for shot 5070. In fact, the numerical coefficient given in Eq. (6) is the resultant value determined by this adjustment. Then this coefficient is fixed both for shots 5070 and 5080 throughout the discharge.

Fig. 3 shows the best fitted simulation results for shots 5070 (closed circle) and 5080 (open circle) and comparisons with experiments (solid lines). Global time behaviour can be well reproduced by the present model. Especially, a remarkable improvement over the previous model is that these reproductions can be obtained with fixed diffusion coefficient over the whole time duration of the discharge both for shot 5070 and 5080. Both plasma profile effects and particle desorption play a role when the particle influx to the wall is reduced. Fig. 4 shows the density profile change in the edge region including SOL at $t = 4$ s (just before gas-puff termination), $t = 5$ and 6 s (1 and 2 s after gas-puff termination) for shot 5070. It is clearly seen that there is a substantial decrease of the density in SOL region after 1 and 2 s (≈40–50%) whereas the average density is reduced only by less than 10–20% (see Fig. 3) at each corresponding time. Fig. 5 shows the time behaviour of the total increment of particle concentration in each of the walls. It is clearly seen that there is some particle desorption from limiter when the particle influx is substantially reduced after gas-puff termination at $t = 4$ s.

It should be noted that, when the plasma conditions are not transient such as in a long pulse steady discharge, profile and desorption effects do not play a major role or these effects can be included by adjusting the particle confinement time. Thus, a more simplified model, like the previous one [1], can still reproduce the experimental results reasonably well.

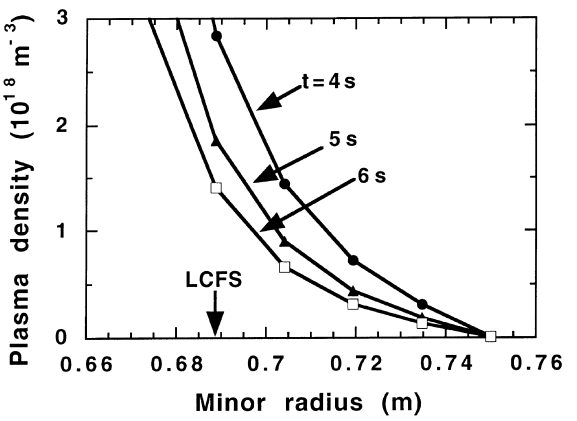


Fig. 4. Time evolution of the plasma density profile near the edge and SOL region at $t = 4$ s (just before gas puff termination), 5 and 6 s (at $t = 1$ and 2 s after gas puff termination) calculated by the simulation for shot 5070. Last closed flux surface is depicted as LCFS.

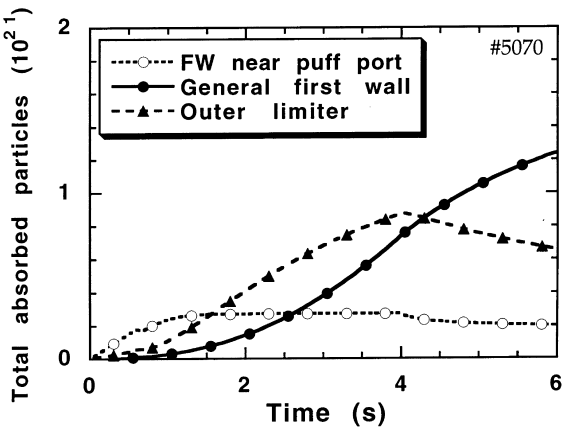


Fig. 5. Time behaviour of total absorbed particles (increment of particle concentration) in the first wall near gas puff port (open circles), the general first wall (closed circles) and the outer limiter (closed triangles) calculated by the simulation for shot 5070.

## 4. Simulation of Tore Supra long pulse experiments

In this section, we will examine the Tore Supra long pulse discharge [11] to identify the dominant wall pumping mechanisms. This discharge was done with lower hybrid current drive with a boronized first wall (shot 9016). The plasma density was maintained almost constant for ≈60 s even under the continuous gas fuelling without actual pumping, so that the walls absorbed all of the fuelled particles. Due to this steady discharge condition, it was deemed to be appropriate to use the more simplified model previously developed [1]. We will introduce two possible absorbing mechanisms in this simplified model: (i) Enhanced diffusion with adsorption along the inner surfaces of the wall, (ii) Enhanced codeposition of hydrogen. The former mechanism has been suggested for the case of boronized wall to explain the enhanced particle release after the shot [12]. Here we will use an effective diffusion coefficient of the first wall and limiter $\approx 3 \times 10^{-17}$ m$^2$/s. For the second mechanism, we will employ the simplified model for the codeposited flux of hydrogen $\Gamma_{\mathrm{NET}}^{\mathrm{co}}$

$$\Gamma_{\mathrm{NET}}^{\mathrm{co}} = \left[ Y_{\mathrm{D}}\phi - \frac{Y_{\mathrm{D}}\phi f_{\mathrm{r}}}{1 - f_{\mathrm{r}} Y_{\mathrm{ss}}}(1 - Y_{\mathrm{ss}}) \right] \frac{N_{\mathrm{c}}}{N_{\mathrm{c\ max}}}, \tag{7}$$

where $Y_{\mathrm{D}}$, $Y_{\mathrm{ss}}$, $f_{\mathrm{r}}$ are the coefficients for hydrogen sputtering and self-sputtering and return fraction of the sputtered atoms [13].

We are interested in the global behaviour of the density and the total number of puffed particles rather than a detailed time behaviour of the gas puff rate and the associated density evolution. Thus, we try to reproduce the time evolution of the total integrated puffed particles when the experimental density behaviour is reproduced by the feedback control of gas puff in the simulation. Fig. 6(a) shows the simulation results for time behaviour of total number of puffed particles with (closed circle) and without (open circle) appropriate enhancement of the diffusion coefficient. In both cases, the experimental time behaviour of total plasma particle can be well reproduced (open square). By choosing the appropriate initial particle concentration in the wall, it is possible to match the total puffed particles at the end of the discharge. However, the global time behaviour of total puffed particles is convex upward in time, which reflect the saturation characteristics in the implantation layer. Fig. 6(b) shows the time behaviour of gas puff rate to reproduce the experimental total plasma particles $N_{\mathrm{p}}$ with enhanced diffusion [closed circle in Fig. 6(a)]. Global features are well consistent with the experiment.

In the case of enhanced codeposition of hydrogen, it has been identified that to reproduce the experimental value of the total puffed particles, fairly low return fraction ($f_{\mathrm{r}} < 0.3$) and large particle flux ($\tau_{\mathrm{p}} < 10$ ms) are required, which seems rather unlikely from the present knowledge of $f_{\mathrm{r}}$ and $\tau_{\mathrm{p}}$. Thus, it is concluded that the codeposition mechanism will play only a limited role in

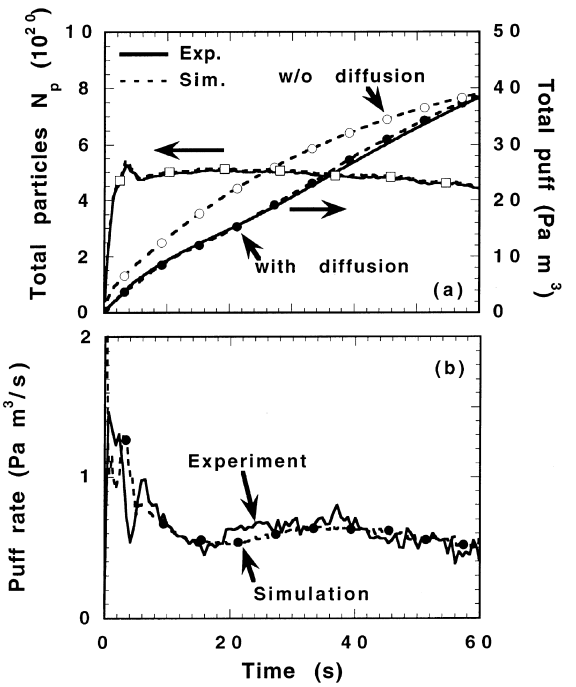


Fig. 6. (a) Time evolution of total puffed particles calculated to match the time behaviour of density (open squares) with (closed circles with dotted line) and without (open circles with dotted line) enhanced diffusion for long pulse Tore Supra discharge (shot 9016). Initial wall concentration is adjusted to match the total puffed particles at $t = 60$ s with the experimental value (solid line). (b) Time behaviour of gas puff rate calculated with enhanced diffusion (solid circles with dotted line) and the experimental value (solid line).

such a large and long time particle absorption observed in the Tore Supra experiments. Further quantitative examination on the role of codeposition is necessary to extrapolate to ITER CFC divertor case, where codeposition is expected to be a dominant mechanism.

## 5. Conclusions

A model to solve the plasma density behaviour coupled with wall pumping/fuelling effect was developed based on an extension of the previous model. In this model, the plasma density behaviour is calculated by a 1-D particle transport model with analytical expression for the neutral source profile to properly describe the density profile effect. The wall model is extended to the one based on the local mixing model to properly include the particle desorption effect. The extended model has been applied to the Tore Supra transition experiment, and is found to reproduce the experimental time behaviour of plasma density reasonably well without any adjustment on the particle confinement time, which was needed in the previous model. However, in the case of steady plasma conditions, it has been shown that the previous model was capable of reproducing essential features. Possible mechanisms for constant pumping of particles in Tore Supra long pulse discharge was examined. Both enhanced diffusion and codeposition were shown to reproduce the experimental results, while more increased enhancement is necessary for the codeposition mechanism.

## Acknowledgements

This report has been prepared as an account of work performed under the Agreement among the European Atomic Energy Community, the Government of Japan, the Government of the Russian Federation, and the Government of the United States of America on Co-operation in the Engineering Design Activities for the International Thermonuclear Experimental Reactor ('ITER EDA Agreement') under the auspices of the International Atomic Energy Agency (IAEA).

## References

[1] M. Sugihara, G. Federici, C. Grisolia, Ph. Ghendrih, T. Loarer et al., 24 th EPS Conference on Controlled Fusion and Plasma Physics, 1997, p. 3–997.
[2] D.K. Brice, B.L. Doyle, W.R. Wampler, S.T. Picraux, L.G. Haggmark, J. Nucl. Mater. 114 (1983) 277.
[3] C. Grisolia, Ph. Ghendrih, B. Pègouriè, A. Grosman, J. Nucl. Mater. 196–198 (1992) 281.
[4] P.K. Mioduszewski, J.T. Hogan, L.W. Owen, R. Maingi, D.K. Lee et al., J. Nucl. Mater. 220–222 (1995) 91.
[5] J. Hogan, IEA Workshop on Tritium Experience in Large Tokamaks, Princeton, 1998.
[6] J.K. Ehrenberg, JET-P(95)18.
[7] J. Ehrenberg, P.J. Harbour, Nucl. Fusion 31 (1991) 287.
[8] S. Rehker, H. Wobig, Plasma Phys. Contr. Fusion 15 (1973) 1083.
[9] P. Andrew, J.P. Coad, J. Ehrenberg, D.H.J. Goodall, L.D. Horton et al., Nucl. Fusion 33 (1993) 1389.
[10] C. Grisolia, L.D. Horton, J.K. Ehrenberg, J. Nucl. Mater. 220–222 (1995) 516.
[11] D. Van Houtte, Equipe Tore Supra, Nucl. Fusion 33 (1993) 137.
[12] C. Grisolia, E. Guthier, A. Grosman, P. Monier-Garbet, E. Tsitrone, 20th EPS Conference on Controlled Fusion and Plasma Physics, Lisbon, vol.II, 1993, p. 595.
[13] G. Federici, C.H. Wu, J. Nucl. Mater. 207 (1993) 62.